PLOS ONE

RESEARCH ARTICLE

Local hydrodynamics at edges of marine canopies under oscillatory flows

Teresa Serra[1]*, **Carolyn Oldham**[2], **Jordi Colomer**[1]

1 Department of Physics, University of Girona, Girona, Spain, **2** Department of Civil, Environmental and Mining Engineering, The University of Western Australia, Perth WA, Australia

* teresa.serra@udg.edu

Citation: Serra T, Oldham C, Colomer J (2018) Local hydrodynamics at edges of marine canopies under oscillatory flows. PLoS ONE 13(8): e0201737. https://doi.org/10.1371/journal.pone.0201737

Editor: Roi Gurka, Coastal Carolina University, UNITED STATES

Received: November 3, 2017

Accepted: July 20, 2018

Published: August 22, 2018

Data Availability Statement: Data are available from the University of Western Australia repository (DOI: 10.26182/5b6d4c6392813 <https://doi.org/10.26182/5b6d4c6392813>).

Funding: Work was supported by the University of Girona funding MPCUdG2016, www.udg.edu, http://research-repository.uwa.edu.au/en/persons/carolyn-oldham(e820ea56-699d-4fb8-97a8-e919b1549c9d).html, and Study Leave Grant from The University of Western Australia to Dr. Teresa Serra, and Ministerio de Economía y Competitividad grant CGL2017-86515-P. The

Abstract

Canopy fragmentation increases both spatial heterogeneity and patch edges which, in turn, is then likely to modify the local hydrodynamics in the canopy. The orientation of the edge versus the wave and current field is also expected to play an important role in determining wave attenuation and sheltering at the edge of a canopy. We investigated the effect a longitudinal edge (i.e. with its main axis aligned to wave direction) of a simulated canopy has on local edge hydrodynamics. The effect that both canopy density and flexibility have on the hydrodynamics was studied. Flexible plants reduced the wave velocity and the turbulent kinetic energy with distance into the canopy and this attenuation increased as the density of the canopy increased. Compared to flexible plants, an edge of rigid plants produced a higher wave velocity attenuation coupled with an increase in the turbulent kinetic energy with distance into the canopy despite having the same canopy density. This greater wave attenuation at the edge coincided with the shifting of the associated mean current that, in turn, produced an increase in the turbulent kinetic energy at the edge in the canopy. The effect was accentuated when the canopy density increased. The wave velocity attenuation was a linear function of the canopy cover. While flexible plants reduced the turbulent kinetic energy following a linear function of the canopy cover, rigid canopies increased the turbulent kinetic energy following a linear function of the canopy cover. In the case of the flexible vegetation, the lengths of both the inner and outer canopy boundary layers increased as the canopy cover increased.

Introduction

Aquatic vegetation plays a critical role in protecting coastal areas. Coastal meadows of aquatic vegetation support infauna [1,2], store carbon [3], reduce erosion [4] and stabilize sediment beds [5], but there are still gaps in the knowledge about the conditions that optimize this function [6]. Bed stabilization in submerged coastal canopies is related to the absorption of kinetic energy by vegetation through a reduction in turbulence [7–10], waves [8,11–13], and mean currents [14,15], and depends on plant flexibility [16], the submergence ratio and canopy density [10,17,18]. As such, unidirectional flow through vegetated canopies has been described by several authors [19,20], where a reduction of up to 90% of the mean flow velocity has been

funders had no role in study design, data collection and analysis, decision to publish, or preparation of the manuscript.

Competing interests: The authors have declared that no competing interests exist.

observed. However, many seagrass meadows are situated in regions dominated by oscillatory flows rather by unidirectional currents. Several authors [4,8,12,13] have investigated the attenuation of both wave velocity and turbulent kinetic energy within a laboratory simulated canopy. Pujol et al [8] compared the ability of flexible and rigid plants to reduce vertical wave velocity and turbulent kinetic energy. While flexible plants always reduced the turbulent kinetic energy, rigid plants with high canopy densities produced an increase in the turbulent kinetic energy in the top layer of the canopy. Wave velocity attenuation by seagrass meadows has been also studied [11,21–23]. A maximum reduction in the wave velocity between 20% and 30% was found inside coastal meadows, compared to immediately above the meadow [22,23]. As a consequence of wave attenuation by canopies, sediment resuspension is reduced [4,5,14,24,25] and particles became trapped, thus increasing water transparency which has an impact on the available light within the canopy [26,27] as well as its global health.

As a result of anthropogenic activities such as anchoring, trawling, fish farming and cables and pipes being laid [28] and also due to the effects of climate change effects [29], total seagrass cover has declined worldwide. As a result canopy fragmentation occurs because mosaics of seagrass patches or canopies with gaps are generated [30]. Low shoot densities, high mortality rates and high fragmentation (the patchiness of continuous habitats) are all indicators of seagrass meadow degradation [31]. Gaps within a canopy leave the bed exposed to both waves and currents and, as such, as they are no longer protected from erosion [32,33] they produce more turbid waters with lower amounts of available light than those in regions covered with vegetation [27,34,35]. The orientation of the canopy gaps (i.e. relative to wave and current direction) is expected to impact the extent of such erosion. The little work that has been done examining differences in orientation suggest that both gap widths and canopy density control the extent of canopy sheltering and therefore the impact the gap's orientation has on erosion. The presence of longitudinal (parallel to the wave/current direction) gaps in a canopy of flexible plants produce a wave penetration within the lateral vegetation, with the extent of penetration being dependent on canopy gap width and canopy density [36]. The presence of transversal (perpendicular to the wave/current direction) gaps within a canopy, produces both wave and turbulent kinetic energy penetration into the nearby lateral vegetation [37]. In both cases, the degree of wave penetration and turbulent kinetic energy attenuation depends on the density of the canopy and the width of the gap. Furthermore, lateral vegetation protects the gap although to what extent depends on both the density of the canopy and the width of the gap [37]. Folkard [38] studied the hydrodynamics in canopies of flexible plants with the presence of transversal gaps and under a unidirectional flow. In his study, the gap aspect ratio and the Reynolds number are the main parameters in determining the type of flow through the canopy and also in which cases the canopy protects the gap.

This work highlighted that canopy fragmentation can lead to habitats that are more vulnerable to external pressures than continuous canopies are. Fragmentation might leave small patches of vegetation disconnected from the canopies. Small patches will have lower canopy densities, shorter leaves and lower nutrient stores than continuous canopies [39], possibly due to the impact of stronger waves and currents experienced within the small patches compared to the large ones.

Fragmentation results in an increase in the number and/or extent of canopy edges and a decrease in inner canopy regions [40]; these edges will experience hydrodynamics that are different to that found within the inner canopy regions. Both waves and turbulence are gradually attenuated across the edge of a seagrass coastal meadow [21]. Nutrient uptake is greatest near the edge of seagrass patches [41], where currents and turbulence are higher than within the canopy. Bowden et al [42] proposed edges as transitional regions between bare sediments and the meadow itself. Ricart et al [43] found that the carbon stocks are 20% higher inside seagrass

patches than at seagrass edges. The presence of an edge of rigid vegetation under unidirectional flow has been studied by several authors [44,45], who found that the mean flow is gradually reduced across the edge of the vegetation (i.e. from the bare soil towards the inner part of the vegetation), producing a shear layer at the canopy edge. Little work has been undertaken investigating hydrodynamics along edges under oscillatory flows.

This study aims to determine the hydrodynamics at canopy edges under an oscillating flow, focusing on canopy edges orientated longitudinally (parallel) to the direction of wave propagation. Furthermore, our study aims to evaluate the horizontal length of the characteristic regions that define the hydrodynamics across the boundary of a canopy of flexible plants. To determine the effect plant stiffness has at the edge of a canopy, the hydrodynamics at the edge of a flexible canopy are compared with those at the edge of a rigid canopy. The results obtained from laboratory experiments are also compared to those obtained in coastal canopies of *Posidonia oceanica* meadows. Here, canopy cover (instead of the canopy density) is considered to compare the laboratory results of our study with those of the coastal canopies.

Materials and methods

The research was carried out in a laboratory flume (6 m long, 0.5 m wide and 0.5 m deep) with a mean water height, h, of 0.3 m (Fig 1A). The flume was equipped with a vertical paddle-type wavemaker at the entrance. The vertical paddle was driven by a variable-speed motor that operated at a frequency of 1.2 Hz. This frequency was chosen to align with previous work [8,9,23,46], and induced 1.03 m wavelengths, corresponding to transitional water waves which are typical in regions dominated by aquatic vegetation. A plywood beach (slope 1:3) was placed at the end of the flume and covered in foam to better attenuate incoming waves, thus ensuring that wave reflection was less than 10% of the incoming wave [8,13]. For further details of the experimental setup see Pujol et al [8]. We defined the longitudinal direction, x, to be zero at the position of the wavemaker in the longitudinal direction, the lateral direction, y, is zero at the centerline of the tank, and the vertical direction, z, is zero at the flume bed (Fig 1A and 1B).

To study edge effects, half the base of the flume was covered with a vegetation plant model (Fig 1B) and the other half was kept free of plants. For this purpose, the base of the flume was covered with 1-cm thick PVC boards perforated with 1cm in diameter holes, in which the plants were placed (Fig 1C). In this study we used two vegetation models, rigid and flexible (Fig 1D) with a height of h_v = 14 cm, and constructed following the details from Pujol et al [8]. The canopy model was placed 1 m away from the wavemaker. Rigid plants consisted of PVC cylinders 1 cm in diameter. Flexible plants consisted of polyethylene blades attached with a plastic band to a PVC dowel (2 cm long and 1 cm in diameter). Empty holes in the PVC boards were filled with dowels (1 cm long and 1 cm in diameter). The flexible model plants were constructed following the methodology of Pujol et al [47], so that they were dynamically and geometrically similar to *Posidonia oceanica* [8,38,48].

The density of the canopy was determined by the Solid Plant Fraction (SPF). The SPF can be defined [10] as the fraction of the bottom boundary occupied by stems SPF(%) = $n_{stems}A_{stem}/A_{total}\times100$, where n_{stems} is the number of stems, A_{stem} is the horizontal area of each stem ($A_{stem} = \pi d^2/4$), where d is the plant diameter and A_{total} is the total horizontal area occupied by the canopy. Four SPF were used for the rigid canopy model (2.5, 5, 7.5 and 10%) and three for the flexible canopy model (2.5, 5 and 10%), with a canopy number density ranging from 320 to 1280 shoots/m^2. The case for SPF = 0% was also studied. Furthermore, the case of a fully vegetated channel was also studied for all the SPF and for the two canopy models, rigid and flexible. The vegetation pattern for each SPF was created at random with a computer function. The

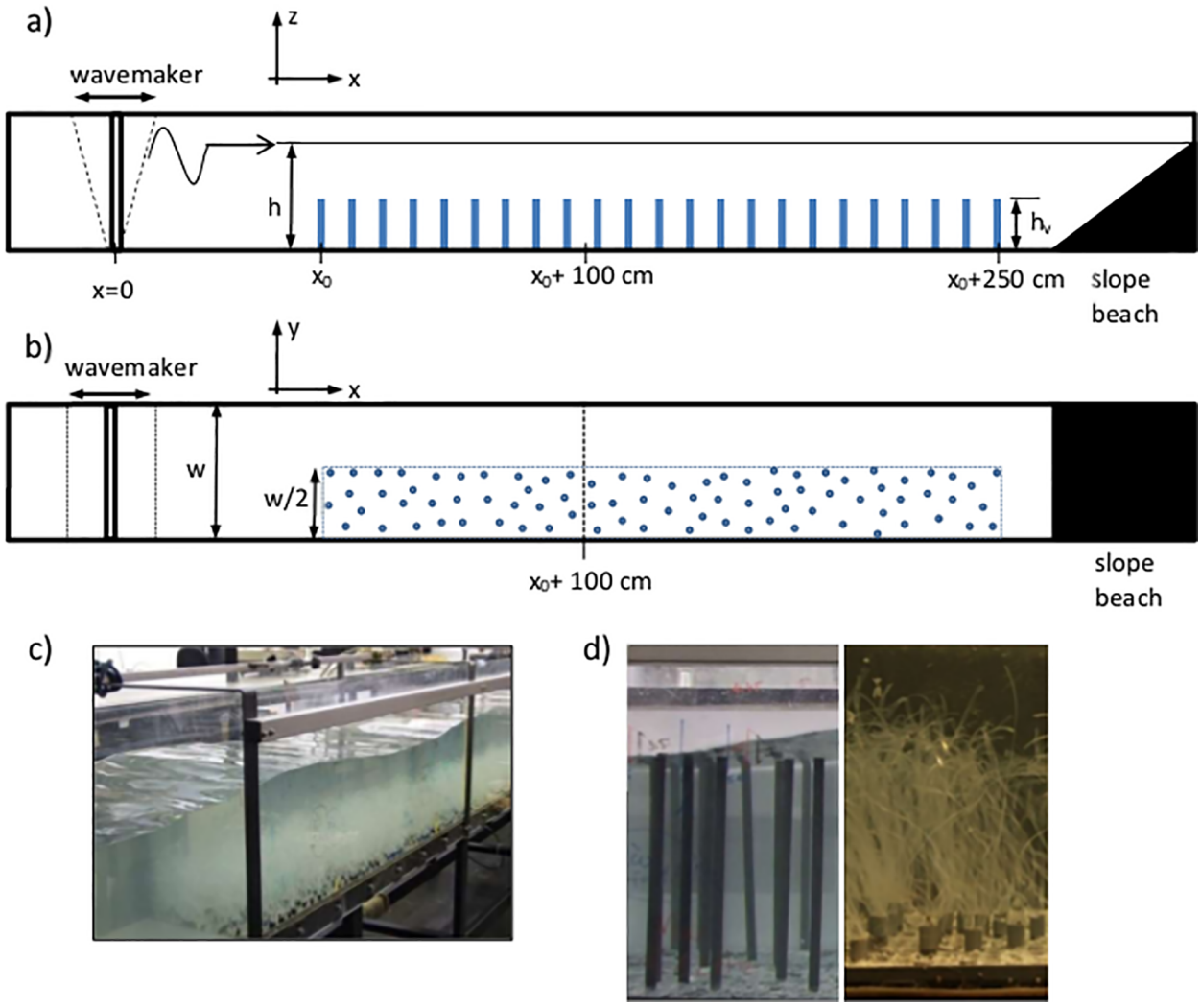

Fig 1. a) Scheme of the side view of the experimental setup. h represents the water height, h_v the vegetation height. b) Scheme of the top view of the experimental setup. c) Photograph of the flume with the distribution of the simulated vegetation. d) Photograph of the plants in the two vegetation models used (rigid and flexible).

https://doi.org/10.1371/journal.pone.0201737.g001

cover of the flexible canopy was obtained from a binarized black and white photograph taken from the top of the canopy (Fig 2) and by using image analysis software with Matlab [10,49,50]. Flexible leaves were painted black and to increase the contrast the PVC bottom was substituted by a white board [50]. Photographs of each flexible canopy density were obtained and analyzed afterwards. The software distinguished between the black and white zones in order to calculate the area of the canopy. The cover obtained for a complete cover of the flume of flexible plants with SPF = 2.5%, 5% and 10%, was 40% (Fig 2A), 60% (Fig 2B) and 80% (Fig 2C), respectively. However, since the flume was half covered (Fig 1A), the cover considered was also half the value obtained for the full cover, i.e., 20%, 30% and 40%, respectively. For the rigid canopy, the cover coincided with the SPF for a full coverage of the flume. Since the flume was half covered, the cover for rigid canopies was half the SPF value in each case, i.e., 1.25%, 2.5%, 3.75% and 5% for SPF = 2.5%, 5%, 7.5% and 10%, respectively.

All measurements were taken in the central y–z plane, at $x = x_0+100$ cm, where x_0 is the position of the beginning of the stem distribution from the wavemaker for all SPF. The same

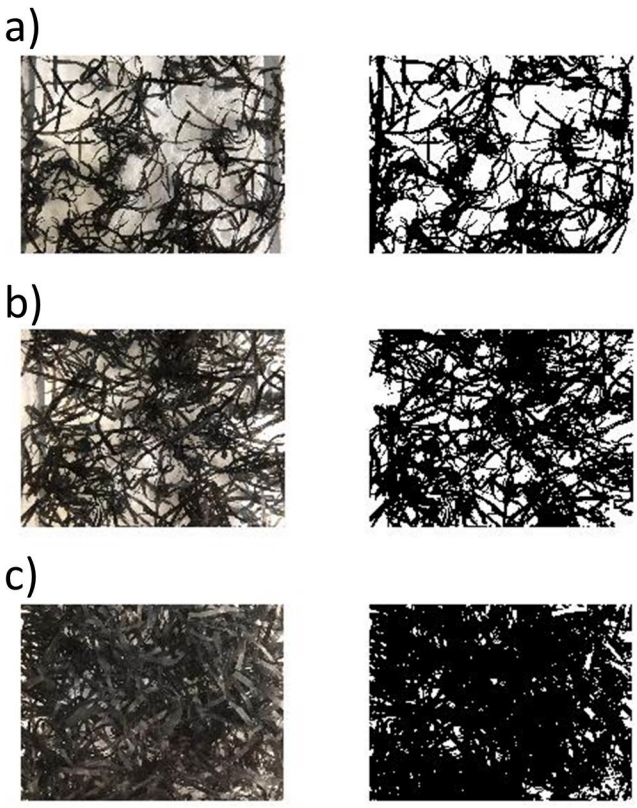

Fig 2. Top view photograph of the flexible canopy (left panels) and black and white digitized image using Matlab software (right panels) of canopy densities of a) SPF = 2.5%, b) SPF = 5% and c) SPF = 7.5%.

https://doi.org/10.1371/journal.pone.0201737.g002

position was also considered for SPF = 0%. Nineteen vertical velocity profiles were measured at different y-positions across the flume, thirteen within the vegetation (-23 cm, -21 cm, -19 cm, -17 cm, -15 cm, -13 cm, -11 cm, -10 cm, -9 cm, -7 cm, -5 cm, -3 cm and -1 cm) and six outside the vegetation (0, 3 cm, 5 cm and 7 cm, 9 cm and 11 cm), where y = 0 cm corresponded to the position of the edge of the vegetation across the width of the flume. For SPF = 0%, the velocity profile was made at the center of the flume (y = 0 cm). The measurements were taken with an Acoustic Doppler Velocimeter (16 MHz-ADV, SonTek Inc.). This instrument records (at 50 Hz) the three instantaneous velocity components at a single-point situated 5 cm from the probe tip using a sampling volume of 0.09 cm^3. The ADV was placed in the flume in a downward looking configuration and connected to a PC with data acquisition software. The ADV instrument was configured to sample over 10-minute intervals (30,000 recordings per sampling interval).

The ADV was mounted in a frame and velocity profiles measured from z = 1 to 20 cm from the bottom of the flume, with a vertical resolution of 2 cm. Velocity measurements near the surface were limited by both wave shape and the 5-cm distance between the ADV sensor and the ADV sampling volume. To avoid spikes, beam correlations lower than 80% were removed. At two vertical positions (z = 8 cm and z = 20 cm above the bottom) low correlation was obtained. These 'weak spots' occurred when the first pulse emitted from the ADV was reflected at the bottom of the flume and met the second pulse within the sampling volume in time and space [8]. As the time lag between pulses depends on the velocity range, the ADV operational range was changed for these points (SonTek YSI, Acoustic Doppler Velocimeter Technical Instrumentation).

To obtain valid data acquisition within the canopy, a few stems were removed to ensure the ADV beam was not blocked and the acoustic receivers and transmitter performed properly [51,52]. To test the effect the 'hole' had on the ambient hydrodynamics, velocities were measured half a centimeter above the top of the canopy, both within and outside the hole. A 3% difference in velocities between 'hole' and 'no hole' canopies was observed at the highest SPF, while only 1% difference was observed at the lowest SPF. We therefore concluded that the 'hole' made minimal modifications to the ambient hydrodynamics.

Method of analysis

In oscillatory flows the instantaneous velocity u can be decomposed into the time-averaged velocity (U_c), orbital velocity (U_w) and turbulent velocity (u') components as:

$$u = U_c + U_w + u'. \quad (1)$$

The above decomposition was made by using a phase-averaging technique [8,13] and the Hilbert transform was used to average oscillatory flow velocities with a common phase (φ). The velocity readings were binned into different phases as described by Pujol et al [9]. The root mean square of u(φ) was then defined as the orbital velocity $U_{w,rms}$ (hereafter denoted U_w) as:

$$U_{w,rms} = \sqrt{\frac{1}{2\pi}\int_0^{2\pi}(u(\varphi) - U_c)^2 d\varphi}. \quad (2)$$

To calculate the turbulent kinetic energy (TKE) profile for stationary velocity records, the instantaneous velocities (u, v, w) at each sampling point were decomposed into the sum of time-averaged velocities (U_c, V_c, W_c), orbital velocities (U_w, V_w, W_w) and the turbulent components (u', v', w') as described in Eq (1). The TKE was calculated as:

$$TKE = 1/2(\overline{u'^2} + \overline{v'^2} + \overline{w'^2}). \quad (3)$$

where $\overline{u'^2}$, $\overline{v'^2}$ and $\overline{w'^2}$ are the time-average of the squared instantaneous turbulent velocities on the three axes, x, y and z, respectively.

Results

The ratio between the wave velocity, U_w for the fully vegetated case and the case without plants ($U_{w,wp}$), was calculated for both rigid and flexible model canopies for the SPF = 10%. The profiles of $\alpha_t = U_w/U_{w,wp}$ for both rigid and flexible canopy models are presented in Fig 3A. From the vertical profiles, two distinct zones can be seen: the zone above the canopy and the zone within the canopy. For both rigid and flexible plants, in the above-canopy zone, the wave velocity ratio was slightly above 1. Within the canopy three layers could be differentiated: a) a *canopy top* layer, b) a *shear layer* situated below the canopy top layer and c) a *canopy bottom layer* below the shear layer. The extent of these layers depended on whether plants were flexible or rigid. In the canopy top layer, α_t remained similar to that measured in the zone above the canopy. This layer was thinner (about 1 cm thick) for the rigid canopy model than for the flexible canopy model (about 5 cm thick). Within the shear layer, α_t decreased gradually with depth, with $\Delta\alpha_t/\Delta z = 0.06\ cm^{-1}$ for the rigid vegetation and $\Delta\alpha_t/\Delta z = 0.04\ cm^{-1}$ for the flexible vegetation. This layer was 7 cm thick for both the rigid canopy model and the flexible canopy model and situated below the canopy top layer. In the canopy bottom layer, α_t was nearly constant with depth down to the bottom. In this layer, α_t attained its minimum value. This layer was 6 cm thick for the rigid canopy model and 3 cm thick for the flexible canopy model. Within the canopy, the wave velocity attenuation was greater for the rigid canopy model than

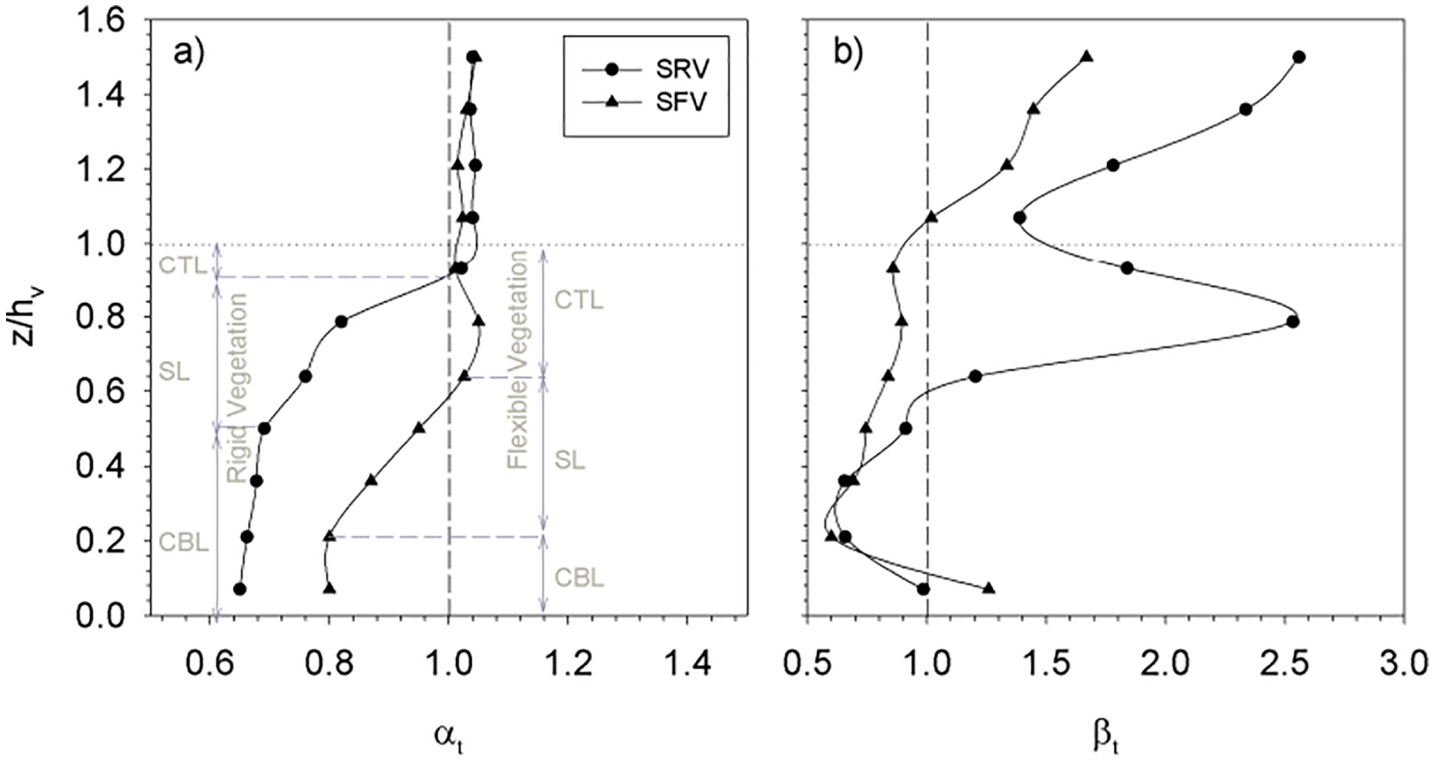

Fig 3. a) α_t profiles at y = 0 cm for the full vegetation case carried out at SPF = 10% for both rigid (SRV) and flexible (SFV) plants. b) β_t profiles at y = 0 cm for the full vegetation case carried out at SPF = 10% for both rigid and flexible plants. Vertical dashed lines represent the ratio $\alpha_t = \beta_t = 1$. Horizontal dotted lines represent plant height. The vertical axis is the non-dimensional height z/h_v above the flume bed. Grey dashed lines represent the vertical layers occupied by the canopy. CTL = canopy top layer, SL = shear layer, CBL = canopy bottom layer.

https://doi.org/10.1371/journal.pone.0201737.g003

for the flexible canopy model (Fig 3A). The ratio between turbulent kinetic energy (TKE) under full canopy coverage (TKE) and without plants (TKE_{wp}) is presented in Fig 3B as $\beta_t = TKE/TKE_{wp}$. For the flexible canopy model, β_t decreased with depth except for the measurement closest to the bottom (at z = 1 cm, Fig 3B). This increase can be attributed to the experimental setup of the flexible plant model that had a small dowel at the base to fix the flexible leaves of the plants. In the above canopy zone, the β_t was greater for the rigid canopy than for the flexible canopy model. At the rigid canopy top layer, β_t presented a maximum, and decreased again in the shear layer. Close to the bottom (at z = 5 cm), both rigid and flexible canopy models had similar β_t.

For the cases with a partial vegetated canopy, we investigated the transversal evolution of U_w, U_c and the TKE in the three canopy layers. To this purpose, three depths were considered within each layer. The depths z = 5 cm, 7 cm and 10 cm were considered to describe the distribution of the wave velocity, the mean flow and the turbulent kinetic energy across the edge of the vegetation. Transects of U_w (Fig 4), U_c (Fig 5) and TKE (Fig 6) across the y direction were plotted for each depth for both rigid and flexible plants at the selected y-locations (see the methods section). The position of the edge of the canopy was situated at y = 0 cm, therefore negative y-values indicate the region within the vegetation model and positive y-values indicate the region without plants. At z = 10 cm, U_w was slightly above $U_{w,wp}$ for the flexible canopy model (Fig 4A) showing the behavior expected in the canopy top layer. In contrast, for the rigid canopy model, U_w at z = 10 cm was already below the $U_{w,wp}$ (Fig 4B), as expected given that z = 10 cm corresponded to the sheared layer for the rigid canopy model. The degree of wave velocity attenuation increased with SPF. For the rigid canopy, U_w and was close to $U_{w,wp}$

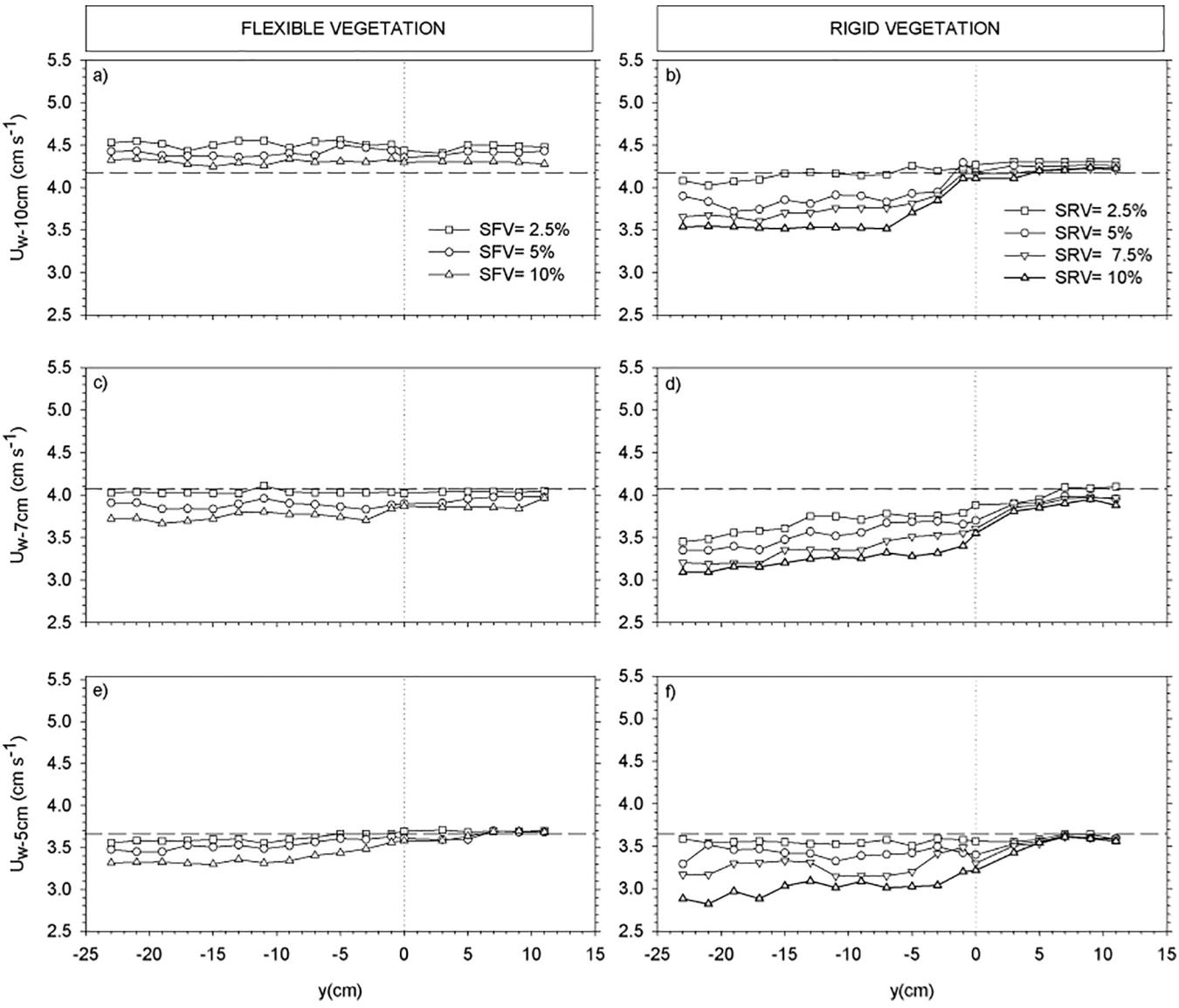

Fig 4. Wave velocity transects across the width of the flume (y-axis) for: z = 10 cm for flexible (a) and rigid (b) canopy models, for z = 7 cm for flexible (c) and rigid (d) canopy models, and z = 5 cm for flexible (e) and rigid (f) canopy models. Horizontal dashed lines correspond to wave velocities for the experiment without plants. Vertical dotted lines correspond to the y-position of the edge of the vegetation. Negative y values correspond to the region covered with plants.

https://doi.org/10.1371/journal.pone.0201737.g004

near the edge within the canopy, and afterwards decreased further towards the inner part of the canopy. Within the canopy at z = 10 cm, the TKE reached a minimum at y = -7 cm and remained constant within the canopy. The depth z = 7 cm was within the sheared layer for both rigid and flexible canopy models. The rigid canopy attenuated waves more than the flexible canopy did, as evidenced by the higher U_w in the flexible canopy model (Fig 4C) compared to the rigid canopy model (Fig 4D). At z = 5 cm, U_w for the flexible canopy model was less than $U_{w,wp}$ (Fig 4E); this was also observed for the rigid canopy model (Fig 4F). The impact SPF had on wave velocity attenuation was greater for the rigid canopy model than for the flexible canopy model. Outside the region covered with flexible vegetation, U_w was close to $U_{w,wp}$ (Fig 4A, 4C and 4E). For rigid plants, U_w outside the vegetated region increased gradually with distance from the canopy edge, with a tendency towards the value of $U_{w,wp}$ (Fig 4D and 4F).

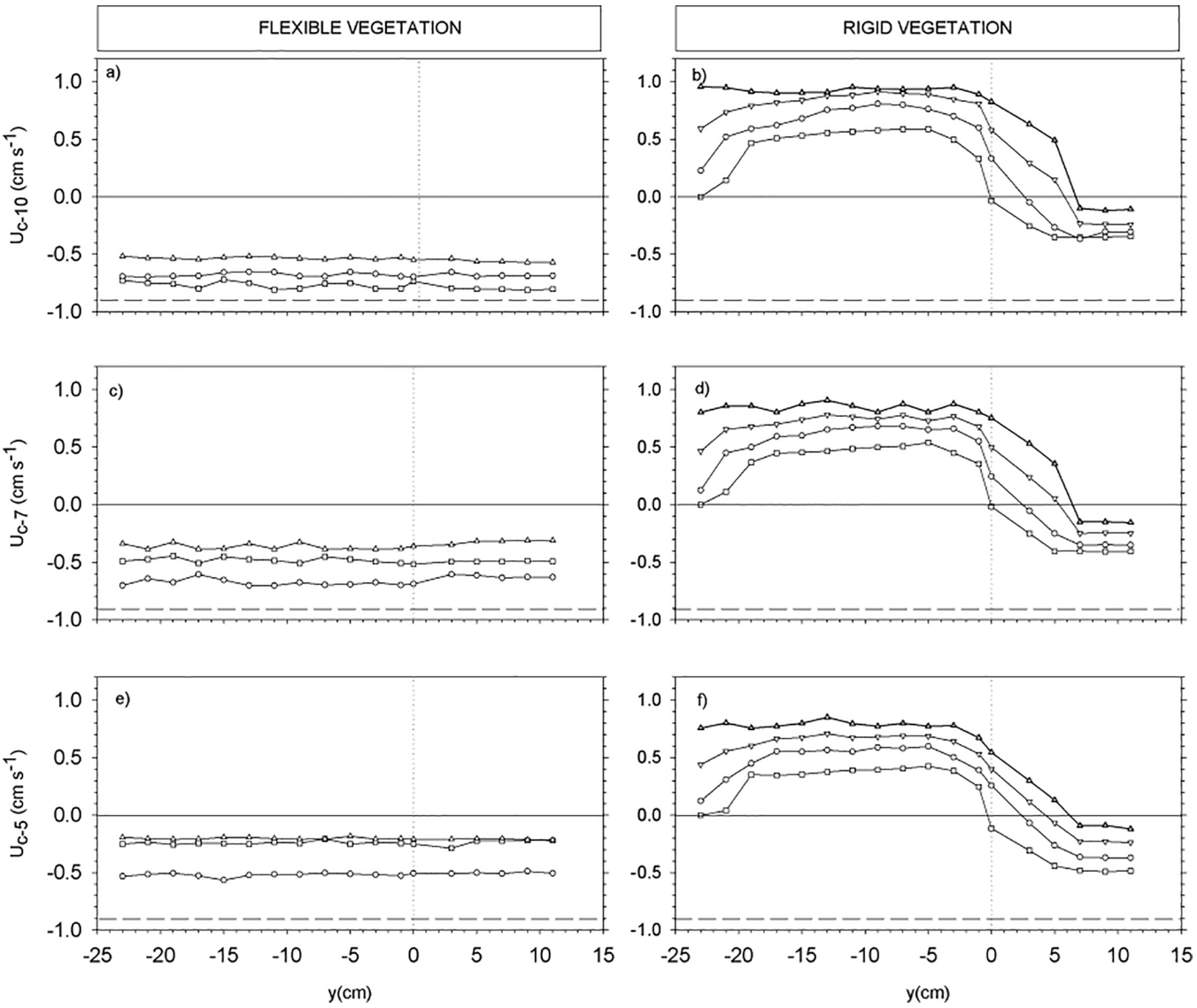

Fig 5. Mean velocity transects across the width of the flume (y-axis) for: z = 10 cm for flexible (a) and rigid (b) canopy models, for z = 7 cm for flexible (c) and rigid (d) canopy models, and z = 5 cm for flexible (e) and rigid (f) canopy models. Positive values indicate flow towards the beach slope while negative values indicate that the flow is directed towards the wavemaker. Horizontal dashed lines correspond to mean velocities for the experiment without plants. Vertical dotted lines correspond to the y-position of the edge of the vegetation. Negative y values correspond to the region covered with plants.

https://doi.org/10.1371/journal.pone.0201737.g005

At z = 10 cm and within the region covered by plants, U_c for the flexible vegetation was smaller than $U_{c,wp}$, but still negative, and flowed in the same direction, i.e., opposite to the wave direction (Fig 5A). The denser the vegetation, the smaller the $U_{c,}$, however, U_c was the same independently of whether the y-position was outside or inside the region covered by flexible plants. In contrast, U_c within the rigid vegetation shifted to positive values, indicating that the flow in this region was in the opposite direction to that measured in the experiment without plants (Fig 5B). U_c outside the rigid vegetated region gradually decreased with distance from the edge, tending towards the U_c measured in the experiment without plants.

The transects of TKE are presented in Fig 6. At z = 10 cm, TKE within the flexible vegetation decreased compared to TKE measured outside the vegetation. The greatest decrease in

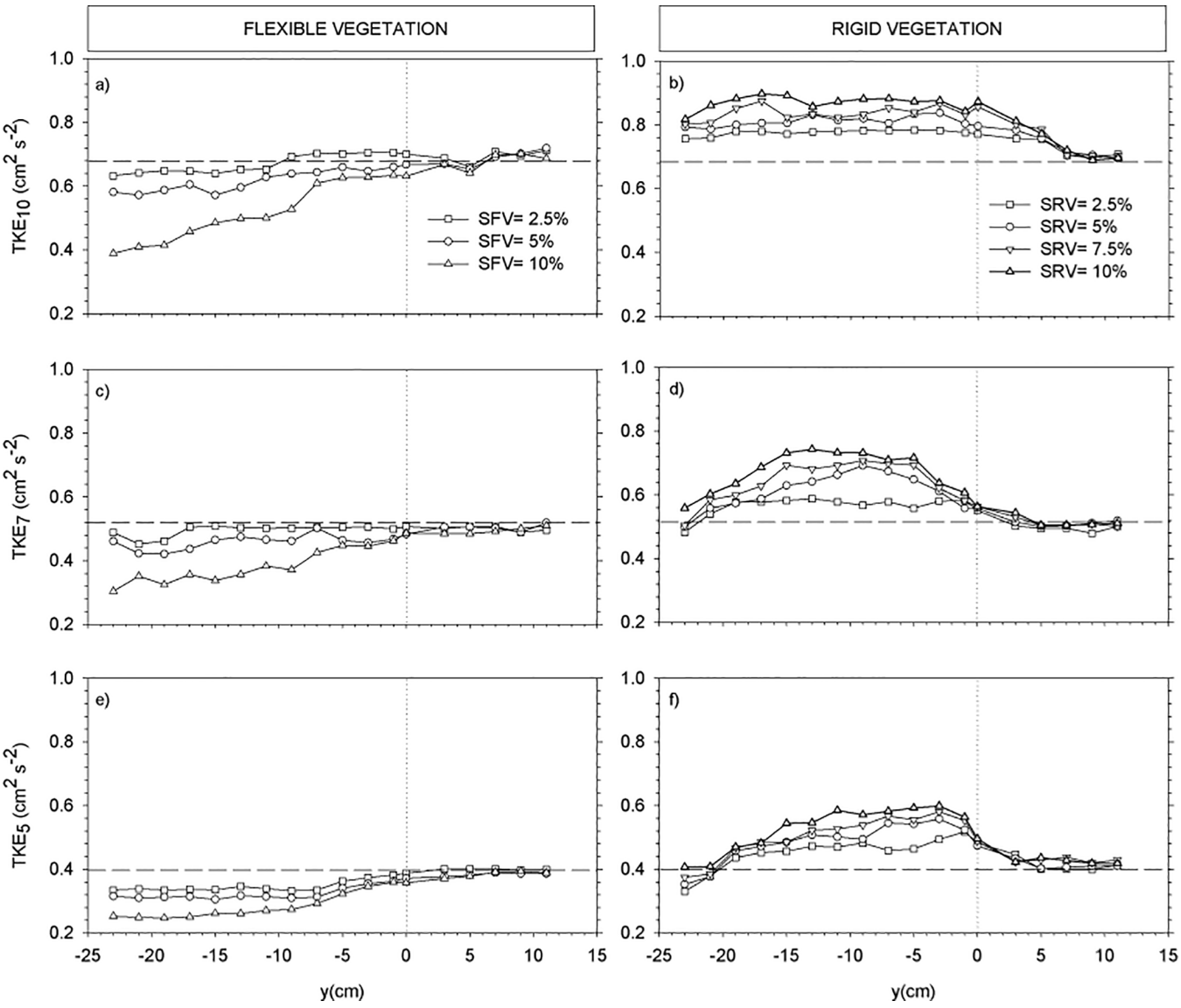

Fig 6. Turbulent kinetic energy transects across the width of the flume (y-axis) for: z = 10 cm for flexible (a) and rigid (b) canopy models, for z = 7 cm for flexible (c) and rigid (d) canopy models, and z = 5 cm for flexible (e) and rigid (f) canopy models. Horizontal dashed lines correspond to turbulent kinetic energies for the experiment without plants. Vertical dotted lines correspond to the y-position of the edge of the vegetation. Negative y values correspond to the region covered with plants.

https://doi.org/10.1371/journal.pone.0201737.g006

TKE was measured at the highest SPF (i.e.10%) (see Fig 6A). For the sparser canopy of 2.5% SPF, the TKE at z = 10 cm was close to TKE_{wp}. At the edge, the TKE was close to TKE_{wp} for all the SPF studied. No reduction in TKE was found outside the vegetated region. In contrast, the TKE within the rigid canopy increased compared to the TKE measured outside the vegetation. The greater the SPF, the higher the TKE inside the vegetation. The TKE at z = 10 cm was nearly constant across the rigid vegetated region. Outside the vegetation, TKE decreased and gradually approached TKE_{wp}. The same patterns of TKE distribution were found at z = 7 cm (Fig 6C and 6D) and at z = 5 cm (Fig 6E and 6F). However, for the rigid vegetation and well inside the vegetated region (from z = -18 cm to z = -23 cm) and at both z = 7 cm and z = 5 cm, the TKE decreased gradually and in some cases at z = 5 cm was less than TKE_{wp} (Fig 6D and 6F).

Discussion

The wave velocity, the mean flow velocity and the turbulent kinetic energy at the longitudinal edge of a simulated meadow have been found to be modified by the flexibility and density of the lateral vegetation for a constant submergence ratio of $h_v/h = 0.47$. The longitudinal edge is thus found to be a region of transition where local hydrodynamics depend on the properties of the canopy. Our results demonstrate consistent modification of the mean flow, the turbulent kinetic energy and the wave velocity across the longitudinal edge of a canopy, suggesting that seagrass canopies have the potential to act as ecosystem engineers and modify local edge hydrodynamics at edges.

Longitudinal edge boundary layers inside canopies: Rigid versus flexible plants

Rigid canopies were found to modify hydrodynamics at longitudinal edges in a different manner to flexible canopies. Wave velocities, U_w, penetrated more deeply into flexible canopies than rigid canopies and, for both canopy types, wave velocities became constant inside the canopy. The attenuation of the wave velocity with distance inside the flexible canopy, induced a reduction in the mean flow velocity, U_c (Fig 5A, 5C and 5E). However, within the rigid canopy, U_c shifted its direction producing a shear layer at the longitudinal edge of the canopy (Fig 5B, 5D and 5F) that resulted in an increase in the TKE. As measured by Pujol et al [8] under full canopy cover (i.e., without gaps), our experiments demonstrated that mean velocities in the top 5 cm of the water column, well above the top of the canopy, flowed towards the beach for both rigid and flexible canopies. Below this layer, but still above the canopy, a return flow directed away from the beach was measured. The direction of the mean velocities inside the canopy was different for flexible and rigid vegetation. Within the rigid canopy, the flow reversed again (positive), which also agreed with Pujol et al [8]. The mean current velocities were also positive over the bare sediment immediately adjacent to the rigid canopy. This pattern of flow within the canopy was different to that found within the flexible canopies. Inside the latter, the mean velocity aligned with flows above the canopy, albeit except for a thin layer at the canopy base. Again, this mirrored the measurements described by Pujol et al [8,9] in an experiment done with fully canopy cover.

In summary, a key feature measured by our experiments was that for the flexible canopy, the direction of the mean flow inside the canopy was the same as outside the canopy (both above and to the side). In contrast, there was a reversal of flows for the rigid canopy (inside versus outside). This produced a horizontal shear layer at the longitudinal edge of the canopy; something which had previously been observed by Nezu and Onitzuka [45] and White and Nepf [53] using a partially vegetated flume with a rigid canopy, but in their case it was under a unidirectional flow.

This shear layer at the rigid longitudinal canopy edge triggered an increase in TKE with distance into the canopy, this effect was accentuated with increasing SPF. This contrasted with the trend of decreasing TKE across the flexible longitudinal canopy edge (see Fig 6A, 6C and 6E), and again this effect was accentuated with increasing SPF.

Hydrodynamic regions across the longitudinal edge of a submerged canopy

The attenuation of both the wave velocity (α_t, Fig 7A) and the turbulent kinetic energy (β_t, Fig 7B) versus the non-dimensional distance y/h_v have been plotted together with the data from Granata et al [11] and Colomer et al [21], both obtained at edges of coastal canopies. During their field survey, Granata et al [11] studied a seagrass canopy with a longitudinal edge, i.e.,

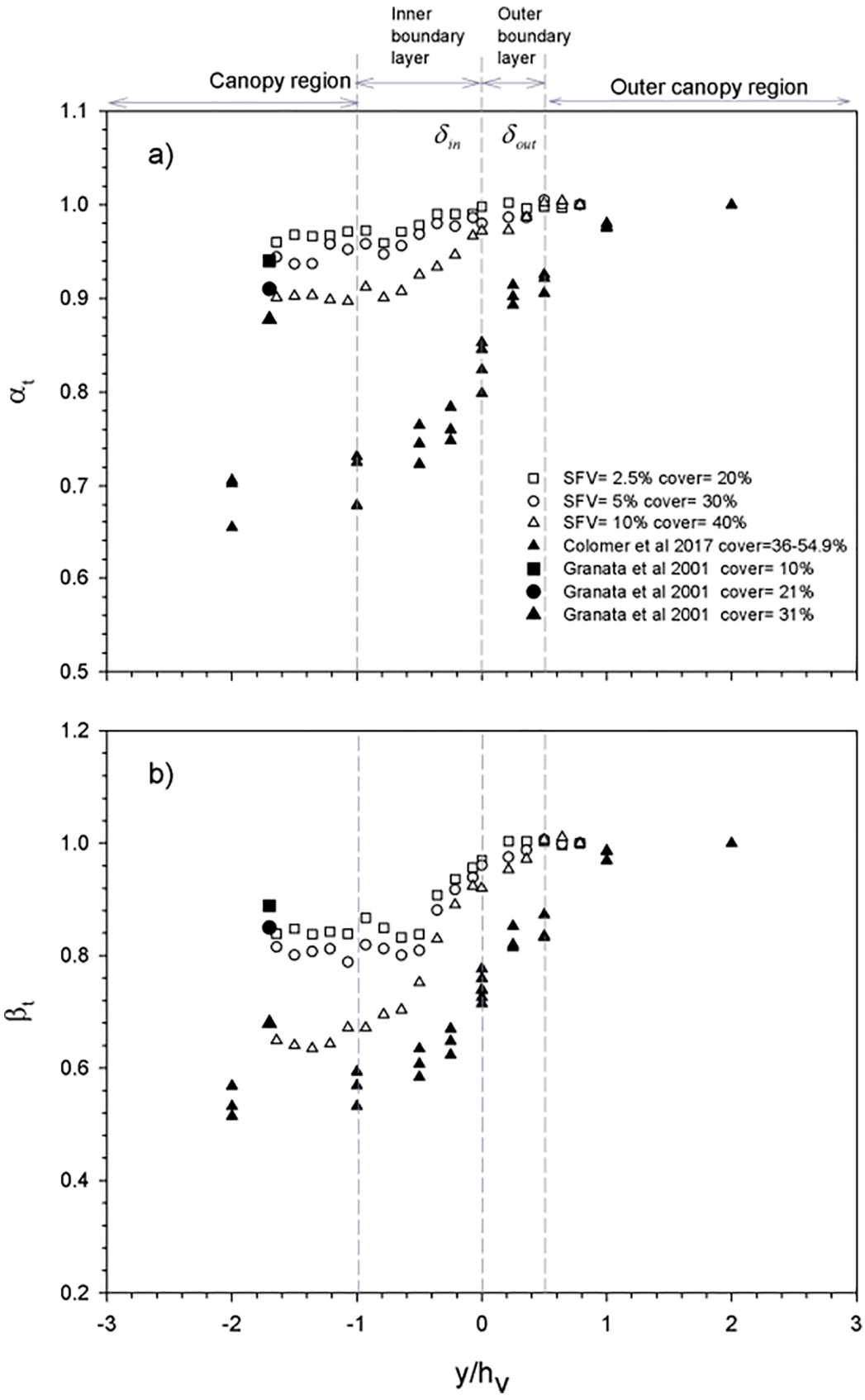
Inner boundary layer
Outer boundary layer
Canopy region
Outer canopy region
a)
δ_{in}
δ_{out}
α_t
SFV= 2.5% cover= 20%
SFV= 5% cover= 30%
SFV= 10% cover= 40%
Colomer et al 2017 cover=36-54.9%
Granata et al 2001 cover= 10%
Granata et al 2001 cover= 21%
Granata et al 2001 cover= 31%
b)
β_t
y/h_V

Fig 7. a) α_t transects across the width of the flume (y-axis) scaled as y/h_v at z = 5 cm above the bottom and for flexible vegetation. b) β_t transects across the width of the flume (y-axis) scaled as y/h_v at z = 5 cm above the bottom and for flexible vegetation. Data from Granata et al [11] and Colomer et al [21] are included. Vertical dashed lines show the limits of the four different zones across the width of the flume, the canopy region, the inner boundary region, the outer boundary layer and the outer canopy region.

https://doi.org/10.1371/journal.pone.0201737.g007

with the main flow direction aligned with the edge. Colomer et al [21] did not specify the main flow direction in any of their surveys, however, the main axis of their gaps were perpendicular to the shore and the predominant wave field in this region is also perpendicular to the shoreline. Therefore, in Colomer et al [21], longitudinal edges could be considered a good approximation. Granata et al. [11], made the velocity measurements within the canopy at $z/h_v = 0.25$. In this present study, measurements were taken at $z/h_v = 0.36$. Therefore, both studies took their measurements within the sheltered layer (Fig 3A), where the wave velocity attenuation is nearly constant. Colomer et al. [21] made the measurements at $z/h_v = 0.42$, slightly above the sheltered layer but still at a depth where the wave velocity remains attenuated (Fig 3A). Combining these field data with our laboratory data, α_t and β_t show that four regions can be distinguished across the longitudinal edge of the canopy. A region outside the canopy (the outer canopy region) where both α_t and β_t are close to 1, indicating a negligible velocity attenuation of both α_t and β_t. An outer boundary layer where both α_t and β_t are below 1 and decreasing gradually towards the longitudinal edge of the canopy, and both α_t and β_t decreasing with the canopy cover. Results from Granata et al [11] and Colomer et al [21] are in accordance with the results presented here. The inner boundary region, where α_t and β_t decrease with distance from the longitudinal edge of the vegetation up to a limit, already in the canopy region with a constant value of α_t and β_t at a distance y that was around the plant height ($\delta_{in} = h_v$); this distance indicates the width of the inner boundary layer inside the canopy. For the same canopy densities, Granata et al [11] found similar α_t and β_t values as those found in the canopy layer at a non-dimensional distance of -1.7 y/h_v within the canopy (Fig 7).

The change of α_t and β_t across the longitudinal edge of a canopy showed that there is a gradual transition in the hydrodynamics from outside the canopy to the inner canopy region. Flexible canopies offer a region where both the turbulent kinetic energy and the wave velocity decrease from the edge of the canopy towards the inner part of the canopy. The boundary is a region in between the inner canopy and the bare soil. The greater levels of TKE and wave velocities compared to those in the inner canopy might produce a greater sediment resuspension and therefore an increase in the turbidity at the boundary, reducing light availability. A reduction in light availability may contribute to producing lower canopy densities at canopy edges when compared to the inner canopies. This effect could help explaining why the biomass of a canopy increases smoothly, rather than abruptly, with distance from the longitudinal canopy edge [54]. Another important factor to consider in determining the biomass of a seagrass across the edge of a canopy is its age. The regions situated at the edge are the younger parts of a seagrass, with a low above- and belowground biomass, while the innermost part of the canopy is the oldeest part with high aboveground and belowground biomass [55].

P. oceanica canopies with canopy covers in the same range as those used here [11] presented similar α_t and β_t values to those obtained in the present study and have been plotted in Fig 7A and 7B, respectively. In our experiments, the flexible canopy of SPF = 2.5% (cover = 20%) produced a lower wave velocity attenuation than that for SPF = 10% (cover = 40%). α_t and β_t values for denser *P. oceanica* canopies with greater covers of 45% [21] have been also plotted in Fig 7A and 7B and presented greater wave velocity attenuations despite having equal shoots per m^2. Therefore, results are in accordance with Paul and Amos [56], who stated that the extent of wave attenuation by the canopy is a function of the canopy density. Luhar et al [13]

studied the wave velocity attenuation by a flexible vegetation in the laboratory with a complete cover of the flume. They found that, at z = 5cm above the bottom, the wave velocity attenuation was $\alpha_t = 0.92$ for a canopy density of 1200 shoots m^{-2}. This result is in accordance with the results found in the present work, where in the inner part of the canopy, the wave velocity attenuation reaches $\alpha_t = 0.9$ for a canopy density of 1280 shoots m^{-2}. In a *Posidonia oceanica* meadow, Infantes et al [57] found a wave velocity attenuation ranging from $\alpha_t = 0.8$ when comparing the wave velocity in the inner canopy with the wave velocity in the location situated closest to a nearby edge of the canopy. For the furthest station from the longitudinal edge, the wave velocity attenuation reached a minimum of $\alpha_t = 0.6$ when compared to the station near the edge. Paul and Amos [56] also stated that the highest wave frequencies were more attenuated than the lowest ones. We did not observe such behavior when comparing laboratory (with f = 1.2Hz) with field (with f~0.25Hz) measurements. However, since different α_t and β_t values were obtained for different canopy covers, but with similar canopy number densities, the canopy cover may be the best indicator of the differences observed in the hydrodynamics of canopy edges.

The length scale of the inner boundary (δ_{in}) was calculated as the length from the longitudinal edge at which U_w and TKE attained a constant value that remained constant within the canopy thereafter (Fig 7). Therefore, δ_{in} was the y value at which the linear trend of both TKE and U_w in the inner boundary layer intercepted the horizontal constant value of U_w and the TKE in the canopy region. The length scale of the outer boundary (δ_{out}) was calculated as the length from the longitudinal edge at which U_w and TKE attained a constant value equal to $U_{w,wp}$ and TKE_{wp}, respectively. Thus, δ_{out} was the y value at which the linear trends at the outer boundary layer of both U_w and TKE intercepted the constant value of $U_{w,wp}$ and TKE_{wp}, respectively. This calculation was done at the measurement point, i.e., 1 m from the beginning of the vegetation. The non-dimensional scales δ/h_v for both the inner and the outer boundary layers versus the cover for the results of the present study and those from Colomer et al [21], for a mean canopy cover of 40% (Fig 8) have been plotted. δ/h_v for the inner boundary layer presented a slight increase with the canopy cover from 0.9 for the experiments carried out in this study to $\delta/h_v = 1$ for the field case carried out by Colomer et al [21]. The inner canopy length scale represents the length up to which the canopy is affected by the nearby bare soil, i.e., where high levels of turbulence and wave velocities prevail. Characteristic values of the scale of the inner boundary layer have been found by other authors studying the biomass of a *Zostera muelleri* seagrass. They found that most of the change in the biomass occurred in the first 0.5 m from the edge of the canopy. Since *Zostera muelleri* seagrass has a mean leaf length of 0.5 m [58] and, based on the biomass change, δ/h_v was close to 1. δ/h_v for the outer boundary layer increased markedly with the canopy cover.

In comparison with the flexible canopy, a longer boundary layer length scale was obtained for the rigid canopy, coinciding also with an increase in the turbulent kinetic energy and a shift in the mean flow from positive values within the canopy towards the bed where the mean flow reaches negative values. The shift in the mean current direction might be similar to the streaming flow produced at boundaries in unidirectional flows [45], which has been also related to an increase in the turbulent kinetic energy at the boundary. However, in a unidirectional flow regime, the flow velocities are usually one order of magnitude greater [53] than the mean flow velocities associated with the wave field that have been found in the present study. The increase in the turbulent kinetic energy might produce erosion of the bed at the longitudinal edges, like those found in the field patches under unidirectional flow for leading canopy edges and longitudinal edges [14]. Bouma et al [14] also found that high canopy densities produced greater erosion at the leading edges than low canopy densities did. In the present study, this might be explained by the larger boundary layer length scale provided by denser canopies

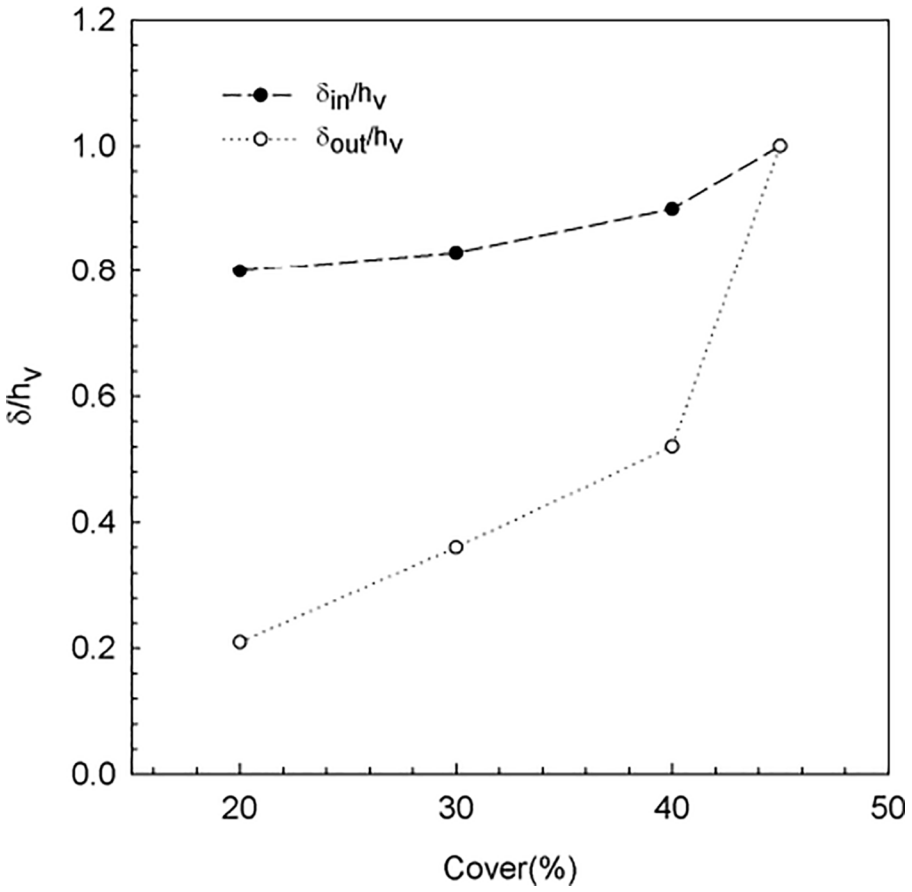

Fig 8. Non-dimensional length (δ/h_v) of the inner and outer boundary layers versus the canopy cover.

https://doi.org/10.1371/journal.pone.0201737.g008

compared to low canopy densities. High levels of turbulent kinetic energy are also associated to a greater sediment resuspension [4,59,60].

The results obtained for α_t and β_t in the longitudinal edge of laboratory simulated canopies were plotted versus the canopy cover in Fig 9A and 9B, respectively. Results for α_t and β_t obtained in field canopies by Granata et al [11] and Colomer et al [21] were also included for completion in the analysis. The canopy characteristics for all the studies considered are listed in Table 1. Data considered corresponded to y-positions inside the canopy greater than $h_v/2$ from the longitudinal edge of the canopy, i.e., falling in the canopy region or close to the canopy region. Results for flexible canopies obtained in the present study, together with those of Colomer et al [21] and Granata et al [11], showed a linear decrease of α_t with the canopy cover, with a slope of -0.651×10^{-2} (Fig 9A). However, the rigid canopies in the present study presented a stronger linear decrease of α_t with the canopy cover, with a slope of -3.889×10^{-2} (Fig 9A), in accordance with the fact that rigid plants produced higher wave velocity attenuations (Fig 4).

El Allaoui et al [36] studied the effect wave penetration has in lateral rigid vegetation near to a longitudinal gap using a similar setup like that used in this present study. They found high wave velocity attenuations of $\alpha_t = 0.62$ and $\alpha_t = 0.67$ for canopy densities of 10% with gap widths of 12.5 cm and 18.75 cm. The greater wave velocity attenuations in their case compared to those obtained here, might be attributed to the small gap used in their studies compared to the size of the bare bed (of 25 cm) used in the present experiment. The lateral vegetation

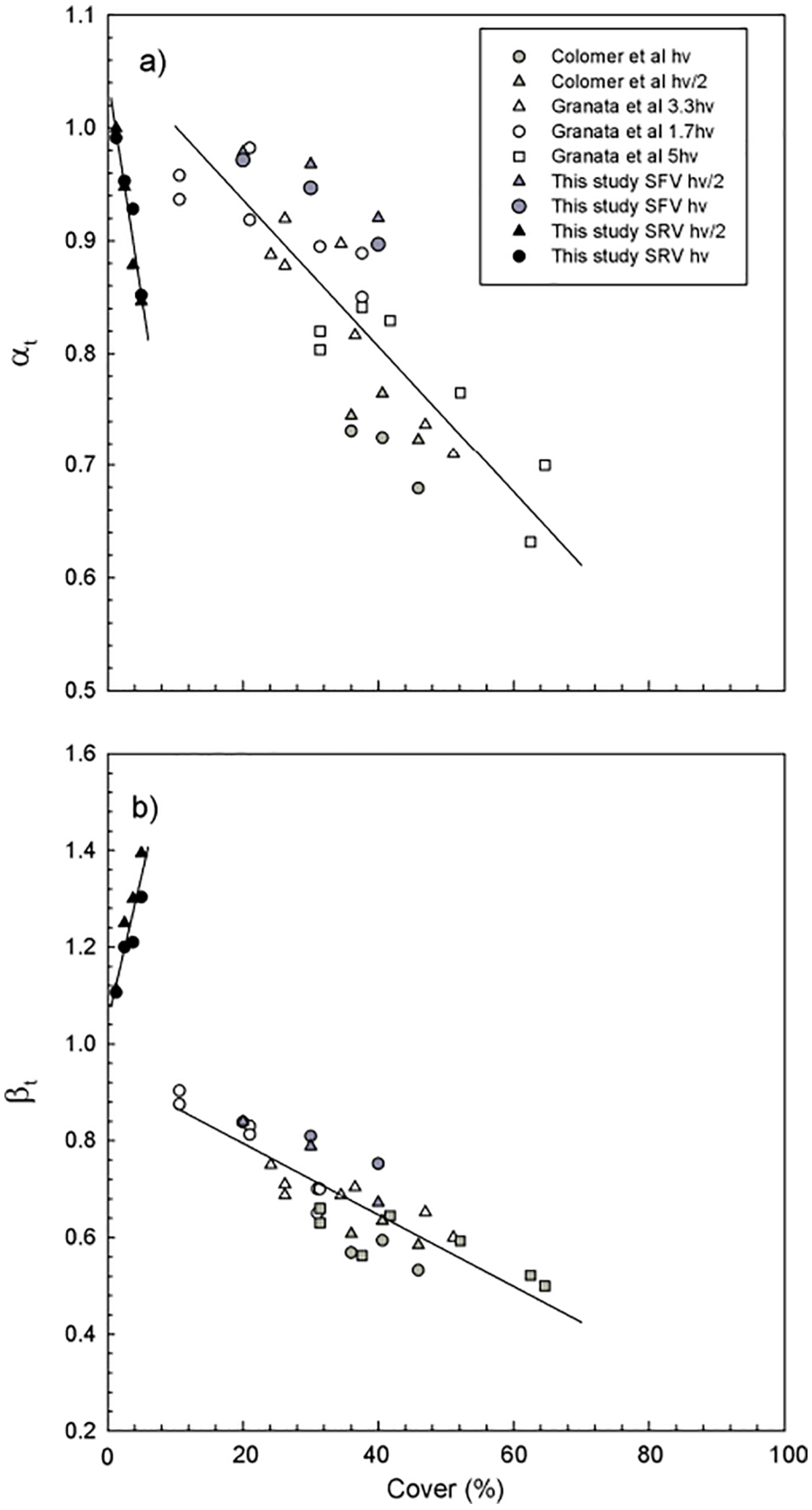
a)
b)
Colomer et al hv
Colomer et al hv/2
Granata et al 3.3hv
Granata et al 1.7hv
Granata et al 5hv
This study SFV hv/2
This study SFV hv
This study SRV hv/2
This study SRV hv
α_t
β_t
Cover (%)
1.1
1.0
0.9
0.8
0.7
0.6
0.5
1.6
1.4
1.2
1.0
0.8
0.6
0.4
0.2
0
20
40
60
80
100

Fig 9. a) Relationship between α_t and the canopy cover for flexible vegetation (with a linear fit $\alpha_t = -0.651\times10^{-2}$cover $+1.066$, $r^2 = 0.684$, 99% confidence) and for rigid vegetation (with a linear fit $\alpha_t = -3.889\times10^{-2}$cover$+1.046$, $r^2 = 0.946$, 99% confidence). b) Relationship between β_t and the canopy cover for flexible vegetation (with a linear fit $\beta_t = -0.739\times10^{-2}$cover $+0.943$, $r^2 = 0.689$, 99% confidence) and for rigid vegetation (with a linear fit $\beta_t = 5.990\times10^{-2}$cover $+1.047$, $r^2 = 0.825$, 99% confidence).

https://doi.org/10.1371/journal.pone.0201737.g009

Table 1. Solid plant fraction range (in %), canopy type, shoots per square meter, cover (in%) for the different experiments carried out (in %) in this study and also for those used for the analysis and comparison.

SPF(%)	Canopy type	Shoots/m^2	Cover (%)	Font
2.5–10	simulated, flexible vegetation	320–1280	20–40	This study
-	*P. oceanica*	231–311	36–54.9	Colomer et al (2017)
-	*P. oceanica*	50–200	10–31	Granata et al (2001)

https://doi.org/10.1371/journal.pone.0201737.t001

Table 2. Solid plant fraction (SPF), vertical wave velocity attenuation (α_w), ratio between the orbital excursion length (A_∞) and the plant-to-plant distance (d), ratio between the plant-to-plant distance (S) and the stem diameter (d) and vegetation type (flexible or rigid).

SPF (%)	$\alpha_w = U_{w,5cm}/U_{w,\infty}$	A_∞/S	S/d	Vegetation type
2.5	0.86	0.12	4.6	Flexible
5	0.82	0.19	3	Flexible
7.5	0.79	0.25	2.2	Flexible
2.5	0.83	0.12	4.6	Rigid
5	0.81	0.19	3	Rigid
7.5	0.76	0.25	2.2	Rigid
10	0.71	0.31	1.8	Rigid

https://doi.org/10.1371/journal.pone.0201737.t002

situated at the two sides of the gap, protected the small gap used by El Allaoui et al [36]. And, conversely, the gap in their case was probably too small to allow the same wave penetration within the lateral vegetation as that in the present study. Folkard [38] also found that the flow penetration within both the gap and the nearby lateral vegetation depended on gap size. The vertical wave attenuation parameter ($\alpha_w = U_{w,5cm}/U_{w,\infty}$, where $U_{w,\infty}$ is the wave velocity far above the canopy and $U_{w,5cm}$ is the wave velocity within the canopy at 5 cm above the bottom) was calculated for the cases studied in the laboratory (Table 2). The values obtained for α_w are in accordance with those obtained by Pujol et al [8] for the same canopy densities and the same range of S/d and A_∞/S (where $S = 1/N^{1/2}$-d is the plant-to-plant distance, $A_\infty = U_\infty/(\omega S)$ is the orbital wave excursion length scale and $\omega = 2\pi f$ is the wave frequency in rad s^{-1}) and are also in accordance with the model proposed by Lowe et al [12].

Flexible canopies also produced a linear decrease of β_t with the canopy cover with a slope of -0.739×10^{-2} (Fig 9B). In contrast, rigid canopies showed a linear increase of β_t with the canopy cover with a slope of 5.990×10^{-2} (Fig 9B). Denser *P. oceanica* canopies have been documented with covers from 25% to 100% [61]. From the linear decrease of α_t and β_t obtained here, a flexible canopy cover of 100% would produce a maximum wave velocity attenuation of 58.5% (i.e. $\alpha_t = 0.415$) and a maximum turbulent kinetic energy attenuation of 79.7% ($\beta_t = 0.203$). Those values would represent the highest attenuation levels achieved by flexible *P. oceanica* canopies. In addition, the canopy cover, rather than SPF, seems to better predict both the wave and the turbulent kinetic energy attenuations within a canopy.

The differences observed between rigid and flexible vegetation highlight that an experimental simulated rigid canopy does not reproduce the hydrodynamics experienced by a flexible canopy. Therefore, as noted by other authors [13,36,62], plant flexibility is a fundamental parameter to be carefully considered when attempting to mimic the environment around aquatic plants in the laboratory. In this present study, the impact on the hydrodynamics of flexible and rigid canopies was studied. Rigid and flexible plants present different hydrodynamics at the canopy edges which also has an impact on the bare soil nearby. In the field, the bending of seagrass plants will vary with season; when leaves are shorter in winter they will behave more like rigid stems whereas in summer, when the leaves are longer, they will bend easily, bringing their movement closer to that observed for flexible plants. Together with our results, this suggests that the hydrodynamic conditions inside the canopy, and along its edges, will vary seasonally, not just in response to seasonal hydrodynamics, but also due to interaction between the life cycle of the seagrass and the modified hydrodynamics.

Acknowledgments

We are grateful to Nazha El Allaoui for her support and help with the experimental data collection. Professor Oldham was supported by a Study Leave Grant from the University of Western Australia. This work was supported by the University of Girona funding MPCUdG2016 and by the Ministerio de Economía, Industria y Competitividad of the Spanish Government through the grant CGL2017-86515-P.

Author Contributions

Conceptualization: Teresa Serra, Carolyn Oldham, Jordi Colomer.

Formal analysis: Teresa Serra, Jordi Colomer.

Investigation: Teresa Serra, Jordi Colomer.

Methodology: Teresa Serra.

Software: Teresa Serra.

Supervision: Carolyn Oldham, Jordi Colomer.

Validation: Jordi Colomer.

Writing – original draft: Teresa Serra.

Writing – review & editing: Teresa Serra, Carolyn Oldham, Jordi Colomer.

References

1. Fredriksen S, De Backer A, Bostrom C, Christie H. Infauna from Zostera marina L. meadows in Norway. Differences in vegetated and unvegetated areas. Mar Biol Res. 2010; 6: 189–200.
2. Hendriks IE, Cabanelles-Reboredo M, Bouma TJ, Deudero S, Duarte CM. Seagrass meadows modify drag forces on the shell of the fan mussel Pinna nobilis. Estuaries and Coasts. 2011; 34: 60–67.
3. Duarte CM. The future of seagrass meadows. Environ Conserv. 2002; 29: 192–206. https://doi.org/10.1017/S0376892902000127
4. Ros À, Colomer J, Serra T, Pujol D, Soler M, Casamitjana X. Experimental observations on sediment resuspension within submerged model canopies under oscillatory flow. Cont Shelf Res. Elsevier; 2014; 91: 220–231. https://doi.org/10.1016/j.csr.2014.10.004
5. Coulombier T, Neumeier U, Bernatchez P. Sediment transport in a cold climate salt marsh (St. Lawrence Estuary, Canada), the importance of vegetation and waves. Estuar Coast Shelf Sci. 2012; 101: 64–75.

6. Bouma TJ, van Belzen J, Balke T, Zhu Z, Airoldi L, Blight AJ, et al. Identifying knowledge gaps hampering application of intertidal habitats in coastal protection: Opportunities & steps to take. Coast Eng. 2014; 87: 147–157. https://doi.org/10.1016/j.coastaleng.2013.11.014
7. Koch E, Ackerman JD, Verduin J, van Keulen M. Fluid dynamics in seagrass ecology-from molecules to ecosystems. In: Larkum AWD, Orth RJ, Duarte CM, editors. Seagrasses: Biology, Ecology and Conservation. Dordretch: Springer; 2006. pp. 199–225.
8. Pujol D, Serra T, Colomer J, Casamitjana X. Flow structure in canopy models dominated by progressive waves. J Hydrol. 2013; 486: 281–292.
9. Pujol D, Casamitjana X, Serra T, Colomer J. Canopy-scale turbulence under oscillatory flow. Cont Shelf Res. 2013; 66: 9–18. http://dx.doi.org/10.1016/j.csr.2013.06.012
10. Pujol D, Colomer J, Serra T, Casamitjana X. Effect of submerged aquatic vegetation on turbulence induced by an oscillating grid. Cont Shelf Res. 2010; 30: 1019–1029.
11. Granata TC, Serra T, Colomer J, Casamitjana X, Duarte CM, Gacia E. Flow and particle distributions in a nearshore seagrass meadow before and after a storm. Mar Ecol Prog Ser. 2001; 218: 95–106.
12. Lowe R, Kossef J, Monismith S. Oscillatory flow through submerged canopies: 1. Velocity structure. J Geophys Res Ocean. 2005; 110: C10016.
13. Luhar M, Coutu S, Infantes E, Fox S, Nepf HM. Wave-induced velocities inside a model seagrass bed. J Geophys Res. 2010; 115: C12005. https://doi.org/10.1029/2010JC006345
14. Bouma TJ, van Duren LA, Temmerman S, Claverie T, Blanco-Garcia A, Ysebaert T, et al. Spatial flow and sedimentation patterns within patches of epibenthic structures: Combining field, flume and modeling experiments. Cont Shelf Res. 2007; 27: 1020–1045.
15. Lefebvre A, Thompson CEL, Amos CL. Influence of Zoostera marina canopies on uniderectional flow, hydraulic roughness and sediment movement. Cont Shelf Res. 2010; 30: 1783–1794.
16. Paul M, Rupprecht F, Möller I, Bouma TJ, Spencer T, Kudella M, et al. Plant stiffness and biomass as drivers for drag forces under extreme wave loading: A flume study on mimics. Coast Eng. Elsevier B.V.; 2016; 117: 70–78. https://doi.org/10.1016/j.coastaleng.2016.07.004
17. Paul M, Bouma TJ, Amos CL. Wave attenuation by submerged vegetation: combining the effect of organism traits and tidal current. Mar Ecol Prog Ser. 2012; 444: 31–44. Available: http://www.int-res.com/abstracts/meps/v444/p31-41/
18. Anderson ME, Smith JM. Wave attenuation by fl exible, idealized salt marsh vegetation. Coast Eng. Elsevier B.V.; 2014; 83: 82–92. https://doi.org/10.1016/j.coastaleng.2013.10.004
19. Nepf HM, Sullivan J a., Zavistoski R a. A model for diffusion within emergent vegetation. Limnol Oceanogr. 1997; 42: 1735–1745. https://doi.org/10.4319/lo.1997.42.8.1735
20. Nepf HM. Drag, turbulence, and diffusion in flow through emergent vegetation. Water Resour Res. 1999
21. Colomer J, Soler M, Serra T, Casamitjana X, Oldham C. Impact of anthropogenically created canopy gaps on wave attenuation in a Posidonia oceanica meadow. Mar Ecol Prog Ser. 2017; https://doi.org/10.3354/meps12328
22. Luhar M, Infantes E, Orfila A, Terrados J, Nepf HM. Field observations of wave-induced streaming through a submerged seagrass (Posidonia oceanica) meadow. J Geophys Res Ocean. 2013; 118: 1955–1968. https://doi.org/10.1002/jgrc.20162
23. Hansen JCR, Reidenbach MA. Wave and tidally driven flows in eelgrass beds and their effects on sediment suspension. Mar Ecol Prog Ser. 2012; 448: 271–287.
24. Gacia E, Duarte CM. Sediment retention by a Mediterranean Posidonia oceanica meadow: The balance between deposition and resuspension. Estuar Coast Shelf Sci. 2001; 52: 505–514.
25. Hendriks IE, Sintes T, Bouma TJ, Duarte CM. Experimental assessment and modeling evaluation of the effects of the seagrass Posidonia oceanica on flow and particle trapping. Mar Ecol Prog Ser. 2008; 356: 163–173.
26. Boudouresque CF, Meinesz A, Lefevre JR. Mapping the marine benthic communities in Corsica .1. The Posidonia oceanica reef of Saint-Florent [Internet]. Annales de l Institut Oceanographique. 1985. pp. 27–38. Available: isi:A1985ALE3400002
27. Adams MP, Hovey RK, Hipsey MR, Bruce LC, Ghisalberti M, Lowe RJ, et al. Feedback between sediment and light for seagrass: Where is it important? Limnol Oceanogr. 2016; 61: 1937–1955. https://doi.org/10.1002/lno.10319
28. Boudouresque CF, Bernard G, Bonhomme P, Diviacco G, Meinesz A, Pergent G, et al. Protection and conservation of Poseidonia oceanica meadows. publisher R and R, editor. Tunis, 1–202.; 2012.
29. Marbà N, Duarte CM. Mediterranean warming triggers seagrass (Posidonia oceanica) shoot mortality. Glob Chang Biol. 2010; 16: 2366–2375. https://doi.org/10.1111/j.1365-2486.2009.02130.x

30. Robbins BD, Bell SS. Seagrass landscapes: a terrestrial approach to the marine subtidal environment. 1994; 301–304. https://doi.org/10.1016/0169-5347(94)90041-8 PMID: 21236866

31. Airoldi L, Beck MW. Loss, status and trends for coastal marine habitats of Europe. Oceanogr Mar Biol An Annu Rev. 2007; 345–405.

32. Pergent G, Bazairi H, Bianchi C. Climate change and Mediterranean seagrass meadows: a synopsis for environmental managers. Mediterr Mar Sci. 2014; 15: 462–473. Available: http://digital.csic.es/handle/10261/92808

33. Montefalcone M. Ecosystem health assessment using the Mediterranean seagrass Posidonia oceanica: A review. Ecol Indic. 2009; 9: 595–604. https://doi.org/10.1016/j.ecolind.2008.09.013

34. Carr J, D'Odorico P, McGlathery K, Wiberg P. Stability and bistability of seagrass ecosystems in shallow coastal lagoons: Role of feedbacks with sediment resuspension and light attenuation. J Geophys Res Biogeosciences. 2010; 115: 1–14. https://doi.org/10.1029/2009JG001103

35. Vacchi M, Montefalcone M, Bianchi CN, Morri C, Ferrari M. Hydrodynamic constraints to the seaward development of Posidonia oceanica meadows. Estuar Coast Shelf Sci. Elsevier Ltd; 2012; 97: 58–65. https://doi.org/10.1016/j.ecss.2011.11.024

36. El Allaoui N, Serra T, Soler M, Colomer J, Pujol D, Oldham C. Modified hydrodynamics in canopies with longitudinal gaps exposed to oscillatory flows. J Hydrol. 2015; 531: 840–849.

37. El Allaoui N, Serra T, Colomer J, Soler M, Casamitjana X, Oldham C. Interactions between fragmented seagrass canopies and the local hydrodynamics. PLoS One. 2016; 11: 1–19. https://doi.org/10.1371/journal.pone.0156264 PMID: 27227321

38. Folkard AM. Hydrodynamics of model Posidonia oceanica patches in shallow water. Limnol Oceanogr. 2005; 50: 1592–1600.

39. Gera A, Pagès JF, Romero J, Alcoverro T. Combined effects of fragmentation and herbivory on Posidonia oceanica seagrass ecosystems. Santamaria L, editor. J Ecol. 2013; 101: 1053–1061. https://doi.org/10.1111/1365-2745.12109

40. Horinouchi M. Review of the effects of within-patch scale structural complexity on seagrass fishes. J Exp Mar Bio Ecol. 2007; 350: 111–129. https://doi.org/10.1016/j.jembe.2007.06.015

41. Morris EP, Peralta G, Brun FG, van Duren L, Bouma TJ, Perez-Llorens JL. Interaction between hydrodynamics and seagrass canopy structure: Spatially explicit effects on ammonium uptake rates. Limnol Oceanogr. 2008; 53: 1531–1539. https://doi.org/10.4319/lo.2008.53.4.1531

42. Bowden D a, Rowden a a, Attrill MJ. Effect of patch size and in-patch location on the\rinfaunal macroinvertebrate assemblages of Zostera\rmarina seagrass beds. J Exp Mar Bio Ecol. 2001; 259: 133–154. PMID: 11343709

43. Ricart AM, York PH, Rasheed MA, Pérez M, Romero J, Bryant C V, et al. Variability of sedimentary organic carbon in patchy seagrass landscapes. MPB. Elsevier Ltd; 2015; 100: 476–482. https://doi.org/10.1016/j.marpolbul.2015.09.032 PMID: 26428624

44. White BL, Nepf HM. Scalar transport in random cylinder arrays at moderate Reynolds number. J Fluid Mech. 2003; 43–79. Available: http://www.scopus.com/inward/record.url?eid=2-s2.0-0041730711&partnerID=40&md5=6e7b631f75b9cc98ea41af35ee9bd658

45. Nezu I, Onitsuka K. PIV measurements of side-cavity open-channel flows—Wando model in rivers. J Vis. 2002; 5: 77–84. Available: http://www.scopus.com/inward/record.url?eid=2-s2.0-23044534320&partnerID=40&md5=05ca7933a239994e38faabbb976632d2

46. Bradley K, Houser C. Relative velocity of seagrass blades: Implications for wave attenuation in low-energy environments. J Geophys Res Earth Surf. 2009; 114: 1–13.

47. El Allaoui N, Serra T, Soler M, Colomer J, Pujol D, Oldham C. Modified hydrodynamics in canopies with longitudinal gaps exposed to oscillatory flows. J hydology. 2015; 114: 1–13.

48. Ghisalberti M, Nepf HM. Mixing layers and coherent structures in vegetated flows. J Geophys Res Ocean. 2002; 107: C2.

49. Neumeier U. Quantification of vertical density variations of salt-marsh vegetation. Estuar Coast Shelf Sci. 2005; 63: 489–496. https://doi.org/10.1016/j.ecss.2004.12.009

50. Ros À. Effects of aquatic vegetation on sediment transport. PhD-Thesis. 2016.

51. Neumeier U, Ciavola P. Flow resistance and associated sedimentary processes in a Spartina maritime salt-marsh. J Coast Res. 2004; 39: 433–439.

52. Neumeier U, Amos CL. Turbulence reduction by the canopy of coastal Spartina salt-marshes. J Coast Res. 2006; 39: 433–439.

53. White BL, Nepf HM. A vortex-based model of velocity and shear stress in a partially vegetated shallow channel. Water Resour Res. 2008; 44. Available: http://www.scopus.com/inward/record.url?eid=2-s2.0-39749128406&partnerID=40&md5=2670578d551640c3e1f33d9a77411c55

54. Tanner JE. Edge effects on fauna in fragmented seagrass meadows. Austral Ecol. 2005; 30: 210–218. https://doi.org/10.1111/j.1442-9993.2005.01438.x

55. Duarte C, Sand-Jensen K. Seagrass colonization: biomass development and shoot demography in Cymodocea nodosa patches. Mar Ecol Prog Ser. 1990; 67: 97–103. https://doi.org/10.3354/meps067097

56. Paul M, Amos CL. Spatial and seasonal variation in wave attenuation over Zostera noltii. J Geophys Res. 2011; 116: C08019. https://doi.org/10.1029/2010JC006797

57. Infantes E, Orfila A, Simarro G, Terrados J, Luhar M, Nepf H. Effect of a seagrass (Posidonia oceanica) meadow on wave propagation. Mar Ecol Prog Ser. 2012; 456: 63–72. https://doi.org/10.3354/meps09754

58. Jones BL, Unsworth RKF. The perilous state of seagrass in the British Isles Subject Category: Subject Areas: Author for correspondence: R Soc open sc. 2016; 3: 1–14. https://doi.org/10.1098/rsos.150596 PMID: 26909188

59. Orlins JJ, Gulliver JS. Turbulence quantification and sediment resuspension in an oscillating grid chamber. Exp Fluids. 2003; 34: 662–677. https://doi.org/10.1007/s00348-003-0595-z

60. Green MO, Coco G. Review of wave-driven sediment resuspension and transport in estuaries. Rev Geophys. 2013; 52: 77–117.

61. Guillén JE, Sánchez JL, Jiménez S, Martínez J, Codina A, Montero M, et al. Evolution of Posidonia oceanica seagrass meadows and its implications for management. J Sea Res. The Authors; 2013; 83: 65–71. https://doi.org/10.1016/j.seares.2013.04.012

62. Bouma T, Friedrichs M, Klaassen P, van Wesenbeeck B, Brun F, Temmerman S, et al. Effects of shoot stiffness, shoot size and current velocity on scouring sediment from around seedlings and propagules. Mar Ecol Prog Ser. 2009; 388: 293–297. https://doi.org/10.3354/meps08130